Observation of Natural Course Characteristics of Bietti Crystalline Dystrophy by Fundus Fluorescein Angiography

Shengjuan Zhang
Beijing Institute of Ophthalmology, Beijing Ophthalmolgy and Visual Science Key Laboratory, Beijing Tongren Eye Center, Beijing Tongren Hospital, Capital Medical University.Hebei Provincial Key Laboratory of Ophthalmology, Hebei Provincial Eye Institute, Hebei Provincial Eye Hospital.

Lifei Wang
Hebei Provincial Key Laboratory of Ophthalmology, Hebei Provincial Eye Institute, Hebei Provincial Eye Hospital.

Zhiqiang Liu
Hebei Provincial Eye Hospital

Huijing Sun
Hebei Provincial Eye Hospital

Qian Li
Beijing Tongren Hospital

Chen Xing
Hebei Provincial Eye Hospital

Zhe Xiao
: Hebei Eye Hospital

Xiaoyan Peng (74000041@ccmu.edu.cn)
Beijing Tongren Hospital https://orcid.org/0000-0002-3946-5724

Research article

Keywords: Bietti crystalline dystrophy, Fundus fluorescein angiography, Disease development

Posted Date: February 16th, 2021

DOI: https://doi.org/10.21203/rs.3.rs-236890/v1

Abstract

Background: Bietti crystalline dystrophy (BCD) is an autosomal recessive genetic disorder that causes progressive vision loss. Here, 12 patients were followed up for 1–5 years with fundus fluorescein angiography (FFA) to clarify BCD disease development and its classification.

Methods: FFA images were collected for 12 patients with BCD who visited our clinic twice or more in 5 years. Peripheral venous blood was collected to identify a pathogenic gene related to the clinical phenotype.

Results: FFA images identified two BCD types. Type 1 showed retinal pigment epithelium (RPE) atrophy at the macular area, followed by choriocapillaris atrophy, then RPE atrophy appeared at the peripheral retina. Type 2 showed RPE atrophy at the posterior pole and peripheral retina, followed by choriocapillaris atrophy around the macula and along the superior and inferior vascular arcades and optic disc nasal side. Then the posterior and peripheral lesions of type 1 and type 2 were extended to the mid-periphery; at last, all the RPE and choriocapillars atrophied, exposed choroid great vessels, but the macular RPE atrophy of type 2 can existed for a long time.

Conclusions: The two different BCD development types provide a better understanding of the phenotype and the progression of the disease for a precise prognosis and prediction of pathogenesis.

Background

Bietti crystalline dystrophy (BCD) is an autosomal recessive retinal dystrophy characterized by numerous tiny sparkling yellow-white spots at the posterior pole of the fundus. The causative gene has been identified as CYP4V2 [1, 2]. In 1937, Bietti first reported three patients with BCD [3, 4]. Since then, research on the disease has continued, but the natural progression and pathogenesis of BCD remains poorly understood. Most previous work has been cross-sectional studies [5, 6, 7, 8], gene research [1, 2, 9, 10, 11, 12], and case reports [13, 14, 15, 16]. Very few of these studies have used fundus fluorescein angiography (FFA) for BCD and the FFA images mostly involve the posterior pole of fundus. Few articles have reported long-term observations of BCD [17, 18, 19], and most of these articles are only case reports and lack comparisons of the before and after examinations. To our knowledge, no studies have used FFA to follow the progression of BCD in patients.

The aim of the present study was to outline the phenotype of BCD more clearly and to obtain a better understanding of the natural course of BCD. Here, we present 12 cases of BCD focusing on the FFA progression with the goal of identifying the features of BCD development.

Methods

Subjects

The implementation of all research methods in this study followed the provisions of the Declaration of Helsinki, the Ethics Committee of Beijing Tongren Hospital, Capital Medical University, and the Ethics Committee of Hebei Provincial Eye Hospital. This study included 12 unrelated Chinese patients who were followed up at our hospital clinic in last 5 years. The clinical characteristics and images of these patients were retrospectively analyzed. For convenience, patients 1–12 were designated P1-12.

This was a retrospective analysis of 24 eyes of 12 unrelated Chinese patients who had visited our hospital clinic twice or more between January 2013 and December 2018. All the patients had consented for mutation screening in our laboratory. Written informed consent was obtained from each patient before drawing peripheral venous blood for genomic DNA extraction and mutation screening of the CYP4V2 gene by direct sequencing, as previously described [20].

Procedures

All patients underwent complete ophthalmic examinations, including best corrected visual acuity (BCVA), slit-lamp microscopy, Goldman tonometry, indirect dilatation fundus examination, and fundus photography (Kowa, Nonmyd 7, Kowa, Japan). The BCVA measurements were converted to the logarithm of the minimum angle of resolution (logMAR) values [21]. FFA images of all the patients were obtained over a 55 × 55° field with a confocal scanning laser ophthalmoscope (Heidelberg Spectralis, Heidelberg Engineering, Heidelberg, Germany). An exception was P6, whose first visit FFA was done over a 50° field with a Topcon retina camera (TRC-50DX, Topcon Corporation, Tokyo, Japan). The FFA images were used to create jigsaws every time and the jigsaws were compared to establish the developmental features of the BCD fundus lesions.

Results

Clinical Presentation and Genetic Diagnosis

The general conditions and genetic diagnosis results for P1–12 are shown in Tables 1 and 2. The mean patient age was 39.75 ± 12.81 years. The mean BCVA of the 24 eyes was 0.95 ± 1.06 logMAR. P5 and P7 had a family history; none of the other patients had a family history. The lefteye of P6 had a choroidal neovascularization (CNV) at the macular area; no CNVs were found in the eyes of the other patients.

Table 1
Clinical data

Patient	Sex	Age	On set age	Yuzawa stage		Duration(year)	logMAR		Types
				First visit	Last visit		OD	OS	
P1	M	38	36	2	2	1	+ 1.7	+ 0.2	1
P2	F	38	37	2	2	1	+ 0.1	+ 0.5	1
P3	M	49	44	2	3	3	+ 0.2	+ 0.4	1
P4	F	45	40	2	3	5	+ 0.3	+ 0.5	1
P5	F	60	55	2	2	5	0	+ 0.1	1
P6	M	30	23	2	3	4	+ 0.8	+ 0.5	2
P7	F	31	20	3	3	4	+ 3.0	+ 3.0	Unable
P8	M	29	25	3	3	2	+ 0.4	+ 0.8	Unable
P9	F	31	25	3	3	5	+ 0.5	+ 3.0	1
P10	F	66	60	3	3	3	+ 3.0	+ 2.0	1
P11	M	26	24	3	3	1	+ 0.3	+ 0.4	2
P12	M	34	31	3	3	2	+ 0.8	+ 0.4	2

Duration: the duration of the first and last FFA examination (shown as years). M, male; F, female;

logMAR, logarithm of the minimum angle of resolution; OD, right eye; OS, left eye; Unable, unable to judge.

Table 2
Genetic and Consanguinity Status

Patient	Genetic Analysis		Consanguinity
	Allele 1	Allele 2	
P1	c.802-8_810del17insGC	c.802-8_810del17insGC	N
P2	c.992A > C, p. H331P	c.992A > C, p. H331P	N
P3	c.802-8_810del17insGC	g.2979A > G; chr4:187115652A > G	N
P4	c.802-8_810del17insGC	c.992A > C, p. H331P	N
P5	c.992A > C, p. H331P	c.571_571delT,p. Y191Tfs*7	Y
P6	c.802-8_810del17insGC	c.802-8_810del17insGC	N
P7	c.802-8_810del17insGC	c.802-8_810del17insGC	Y
P8	c.802-8_810del17insGC	c.1091-2A > G; g.17344A > G, rs199476183	N
P9	c.958C > T, p. R320X	c.1091-2A > G; g.17344A > G, rs199476183	N
P10	c.802-8_810del17insGC	c.1199G > T, R400L	N
P11	c.802-8_810del17insGC	c.802-8_810del17insGC	N
P12	c.802-8_810del17insGC	c.332T > C; p. I111T	N

N, no; Y, yes.

The severity of fundus appearance was graded at each patient's first visit according to the stages set by Yuzawa et al 22 (for convenience, we call these stages Yuzawa staging). Stage 1 (none of our patients): retinal pigment epithelium (RPE) atrophy with uniform fine white crystalline deposits is observed at the macular area. Stage 2 (P1–6): RPE atrophy extends beyond the posterior pole; choriocapillaris atrophy, in addition to the RPE atrophy, appears markedly at the posterior pole. Stage 3: RPE-choriocapillaris complex atrophy is observed throughout the fundus (P7–12). Three patients (P3, P4, and P6) had progressed to stage 3 at the last visit (Table 1).

Fundus Color Photography

The total number of crystalline deposits decreased over time in all eyes. At the first visit, the posterior pole retina showed dirty bluish gray. At the last visit, the dirty bluish gray of retina was diminished gradually. And the choroidal great vessels were clearer than before. More pigment clumps were apparent (P1-5) (Fig. 1A, B). In P6, P11, P12, the condition of the macular area showed no significant change, but the RPE–choriocapillaris complex of the area around it was more atrophied than before (Fig. 1C, D). A scar cause by choroidal neovascularization was observed at the macular area in the left eye of P6 (Fig. 1F);

this had not been evident at the first visit (Fig. 1E). At the last visits of P7-10, both eyes showed more pigment clumping and the choroidal great vessels were more apparent than at the first visit (Fig. 1G, H).

Fundus Fluorescein Angiography (ffa)

The fluorescence of both eyes in all patients was similar, except the left eye of P5 had a branch retinal vein occlusion and the left eye of P6 had a CNV. In this study, the FFA images at theearly phases revealed hypo-fluorescence due to a filling defect of the choriocapillaris. The hypo-fluorescent lesions showed filling of the choroidal great vessels. The FFA images at the late stage indicated hyper-fluorescence staining of the hypo-fluorescent lesions margin. The mottled fluorescence in this study indicated RPE atrophy, which Mataftsi et al 5 had called a “salt and pepper appearance.”

At their first visits, P1–P4 showed patchy hypo-fluorescence at the macular region and mottled fluorescence around it. The peripheral retina also showed mottled fluorescence, while the mid-peripheral retina showed normal retinal fluorescence (Fig. 2A, Fig. 4A). Mottled fluorescence was observed at the nasal side of P1, while P2 had mottled fluorescence and patchy hypo-fluorescence at the nasal retina and mottled fluorescence at the superior and inferior mid-periphery; however the degree of disorder of the mottled fluorescence was slighter in the superior and inferior mid-periphery than in the posterior pole and periphery, normal retinal fluorescence was only observed at the temporal mid-periphery. At the last visits by P1–P4, the macular and peripheral lesions had extended to the mid-periphery and the RPE atrophy had progressed to choriocapillaris atrophy. This RPE-choriocapillaris complex atrophy was observed throughout the fundus images from P3 and P4 (Fig. 2B, Fig. 4C).

At the first visit by P5, patchy hypo-fluorescence was observed at the macular region, with mottled fluorescence around it, whereas the mid-peripheral and peripheral retinal regions showed normal fluorescence. The left eye of P5 had a branch retinal vein occlusion (Fig. 2C). At the last visit of P5, the lesion of the posterior pole had extended, as had the hypo-fluorescence, and patchy mottled fluorescence was now apparent at the peripheral retina. Points of laser photocoagulation were observed at the branch retinal vein occlusion area of the left eye (Fig. 2D).

At the first visit by P6, the posterior pole and the peripheral and optic disc nasal side retina showed mottled fluorescence, and a few patchy areas of hypo-fluorescence were observed at the nasal and superior nasal areas of the optic disc. The mid-periphery, except for the nasal side, showed normal retinal fluorescence (Fig. 3A, C). A CNV fluorescence was observed at the macular area of the left eye (Fig. 3C), but no treatment was given. At the last visit, the posterior pole and peripheral lesion had extended to the mid-periphery and choriocapillaris atrophy had appeared around the macular area, equivalent to the superior and inferior vascular arcade areas and the optic disc nasal area. At the same time, RPE atrophy had progressed to choriocapillaris atrophy, but the macular RPE atrophy showed no significant changes (Fig. 3B). The CNV fluorescence of the left eye progressed to fluorescence staining of the scar, with annular hypo-fluorescence observed around it (Fig. 3D).

At the first visits by P7 and P8, only few areas of mottled fluorescence remained in the peripheral retina and the superior temporal retina of the optic disc. Most of the fundus was hypo-fluorescent, and the fluorescence of choroidal great vessels were exposed (Fig. 4D). At the last visit, the fundus hypo-fluorescence was extended, the choroidal great vessels were clearer, and the mottled fluorescence area was reduced (Fig. 4F).

At the first visits by P9 and P10, large areas of hypo-fluorescence were seen in the posterior poles of both eyes, with the rest of the area showing mottled fluorescence (Fig. 2E). Patchy hypo-fluorescence was observed at the nasal retina in both eyes of P10. At the last visit, the hypo-fluorescence had expanded and the area of mottled fluorescence was reduced (Fig. 2F).

At the first visits by P11 and P12, the macular region showed mottled fluorescence, withpatchy hypo-fluorescence observed around the macular area (Fig. 3E). The hypo-fluorescent area was larger in P11 than in P12. At the last visit, no macular area changes were evident, and the rest of the retina showed expanded hypo-fluorescence and a more disordered mottled fluorescence (Fig. 3F).

Discussion

The natural progression of BCD remains poorly understood, with few follow-up cases appearing in the published literature. The previous staging methods for BCD have included the Yuzawa staging [22], fundus fluorescein angiography staging [5], and electrophysiological staging [20]. The Yuzawa staging is widely used [5, 20, 23, 24, 25, 26], but most of these studies have been cross-sectional ones or case reports with only small numbers of observed cases. We followed up 12 patients with BCD to determine the natural progression of the disease, and our discussion focuses on the breadth and depth of the fundus lesion of BCD.

Our first focus is on the sequence of BCD lesion occurrences. We found that the posterior pole retina was the first to be attacked, followed by the peripheral retina. Both the posterior and peripheral lesions extended to the mid-periphery, finally all the retina was attacked. The disease progresses more rapidly on the nasal side retina of optic disc, whereas the retina in the mid-peripheral part of the temporal side of the macular area is involved last.

The Yuzawa staging is used widely and divides the disease into three stages. However, these stages were based on three patients, with only one patient followed up for five years, and lesions have occurred throughout the fundus of this patient at the initial visit. The two other patients were cross-sectional observations. They described the first stage of the lesion confined to the macular area, the second stage beyond the posterior pole, and the third stage involving the totalretina. This description tends to give the impression of a centrifugal expansion.

Many subsequent studies have stated that “Yuzawa described a centrifugal expansion of the RPE-choriocapillaris complex atrophy, from the macular area towards the periphery, occurring in three stages” [5, 20, 24, 27], and they agreed with this description. By contrast, our observations were different. In our

opinion, the reasons for this difference were the small case numbers in the previous studies, with even fewer cases of total retinal observation, and a focus of attention on the changes in the posterior pole retina.

Halford et al [27] reported that atrophy of areas of the RPE and choroid tended to develop at the posterior pole, became confluent, and expanded centrifugally to involve peripheral retina, but they only observed a 55° autofluorescence in the fundus images, not a total retinal involvement. Consequently, the conclusion that BCD is a centrifugal expansion disease is questionable. Mataftsi et al [5] conducted jigsaw observations in six patients, but all were advanced cases. According to the Yuzawa staging, all patients were stage 3 and had complete retinal involvement, so the conclusion that BCD is a centrifugal expansion was not justified. However, Mataftsi et al [5] found one patient with mild disease that showed a significant difference, as atrophic changes in the choriocapillaris were evident not only in the posterior pole but also at the equator level, at the eccentricity of the vortex veins. This finding was consistent with our observation: the atrophy in the posterior pole and peripheral choroid appeared before the mid-peripheral atrophy. Mataftsi et al [5] also performed an FFA staging of BCD, but the number of cases was small and all cases were advanced. Therefore, this FFA staging was not comprehensive and will not be discussed further in this article.

Some reports have suggested a centrifugal expansion of the visual defect based on the centralscotoma seen with the 30° visual field test [1, 20, 28]. However, Liu et al [29] confirmed the visual field features using the 85° visual field test. They found that the peripheral and central scotomas initially appear, but as the disease progresses, these expand and combine, ultimately resulting in visual islands only in the mid-periphery, which are not found centrally. This is consistent with our observation of lesions occurring first in the center and periphery and then eventually extending to the mid-periphery.

In this study, we also used the Yuzawa staging, regarding it as a cross-sectional staging method according to the width and depth of the BCD lesions. We simplified the Yuzawa staging as follows: stage 1 consisted of a lesion confined to the posterior pole with only RPE atrophy; stage 2 consisted of a lesion beyond the posterior pole or with choroid atrophy; and stage 3 consisted of total retinal involvement. Since the Yuzawa staging has been used widely for a long time, the application of Yuzawa staging in this study was intended as a convenience for readers to understand the condition of the eyes of our patients. It was not meant to indicate the natural progression of the disease.

We also examined the atrophy sequence of the BCD lesions and found two patterns of BCD atrophy. Type 1 showed RPE atrophy at the macular area, followed by choriocapillaris atrophy at the macula, then RPE atrophy at the peripheral retina, and subsequent extension of the macular and peripheral lesion to the mid-periphery; at the same time, the RPE atrophy extended to choriocapillaris atrophy and eventually all the RPE and choriocapillaris atrophied, exposing the choroid great vessels. Type 2 showed RPE atrophy at the posterior pole and peripheral retina, followed by choriocapillaris atrophy around the macular area, along the superior and inferior vascular arcades, and at optic disc nasal side. Subsequently, the posterior lesion and peripherallesion extended to the mid-periphery, with simultaneous transition of the RPE

atrophy to choriocapillaris atrophy and, ultimately, full RPE and choriocapillaris atrophy, with exposure of the choroid great vessels, but the RPE atrophy of macular can persist for a long time. However, we found that the last area of atrophy at the most advanced stage of BCD was in the temporal peripheral retina, rather than the retinal area last attacked in the mid-periphery.

Mataftsi et al [5] found that peripheral retinal atrophy was relatively mild in the final stage of the disease, which is consistent with our findings. They hypothesized that the posterior ciliary arteries are selectively affected, whereas the anterior uveal circulation (ciliary body and anterior choroid) is preserved until late in the disease, although nevertheless insufficient for supplying the retro-equatorial choroid. We agree with this hypothesis, but it needs further confirmation.

Immunohistochemistry analyses have revealed that CYP4V2 is highly expressed in the choroid and the RPE, while relatively less expressed in the retinal outer and inner nuclear layers, retinal ganglion cells, and corneal epithelial cells, in accordance with the BCD phenotype [30]. The FFA images revealed changes mainly in the RPE and choroid, so RPE dysfunction has been considered the primary change in BCD [20, 27, 31]. One view holds that vascular endothelial growth factor (VEGF) is produced by the RPE and is necessary for choroidal maintenance [32]; therefore, a lack of VEGF caused by an RPE disorder may play a role in choroidal thinning. Our FFA results showed that RPE atrophy occurs first, followed by choroidal vessels atrophy, in agreement with the previous research, including the research by Yuzawa et al [22].

We re-examined the FFA images in the previous literature, and we found that those images can be divided into the two atrophy types we have mentioned here. Type 1 shows choriocapillaris atrophy first appearing at the macula [7, 11, 27, 33, 34], and type 2 shows choriocapillaris atrophy firstappearing around the macular area and along the superior and inferior vascular arcades and optic disc nasal side [7, 15]. The case numbers are significantly smaller for type 2 than for type 1; for example, Wang et al [7] reported that, of the 4 patients examined, 3 were type 1 and 1 was type 2. In the present study, only 3 (P6, 11, and 12) of the 12 cases were type 2. Apart from the macular area changes caused by CNV of P6 left eye, the macular area of the other 5 eyes of the 3 cases showed slow changes and the RPE and choroid atrophy of the mid-periphery and periphery was significantly aggravated. This suggests that the type 2 patients can preserve better vision for a longer time, so these pattern differences may aid in the evaluation of a patient's prognosis.

The reason for these two different atrophy patterns is unknown. We looked at the gene mutation sites of P6, P11, and P12 and found that the P6 and P11 had homozygous mutations of c.802-8_810del17insGC, while P12 was heterozygous for a mutation of c.802-8_810del17insGC and c.332T > C; p. I111T. In this study, P1 and P7 also had homozygous mutations of c.802-8_810del17insGC, but their phenotypes differed from those of P6 and P11 (Table 2). Therefore, the specific causes of these differences need further observation and research.

In the early stage of BCD, distinguishing the progression type is not possible in eyes with disordered pigment epithelium and no choroid atrophy. Only patients with choriocapillaris atrophy can be typed. The type of progression also cannot be determined in patients at the end stage of the disease because the

choriocapillaris and RPE are atrophied and no longer visible, leaving only the image of the choroidal great vessels. We propose adding the progression types to the staging criteria to provide a clearer understanding of how the disease progresses, without creating the misconception that the disease develops in a centrifugal way. The progression type cannot be distinguished in the early and the last stages, but the addition of progression typing, when possible, can help to clarify the characteristics of disease development, while providing a more accurate prognosis and a better understanding of the pathogenesis of BCD.

This study had several limitations, including the small number of included eyes and the lack of primary patient observations. However, considering the rarity of the disease and our review of the previous literature, our study on the progression of BCD using FFA picture jigsaws provides one of the largest collections of images and the largest number of patients. Finding BCD patients with early stage disease is difficult because the visual acuity of patients at this stage is not substantially damaged, so they seldom come to the hospital.

Conclusions

The natural progression of BCD shows two patterns. The reasons for these different types of development need further study, but this study provides a better understanding of the phenotype and the development of the disease. The findings presented here will be helpful for future pathogenesis research and for prognosis assessment of patients with BCD.

Abbreviations

BCD: Bietti crystalline dystrophy; FFA: Fundus fluorescein angiography; RPE: Retinal pigment epithelium; BCVA: best corrected visual acuity; logMAR: logarithm of the minimum angle of resolution; CNV: choroidal neovascularization; VEGF: vascular endothelial growth factor

Declarations

Acknowledgments

Not applicable.

Authors' contributions

SJZ, ZQL, HJS, CX, QL and ZX performed the initial clinical database search, identified confirmed cases of BCD, collected all images as presented. SJZ produced the first draft of the manuscript and figures. XYP, LFW and SJZ contributed to the study concept and design, reviewed all the images and statistical analysis and edited the manuscript, contributing to the final version sent for approval.

Funding

The authors did not receive any grant or funds in support of this study.

Availability of data and material

The datasets used and/or analysed during the current study are available from the corresponding author on reasonable request.

Ethics approval and consent to participate

This study was approved by the Ethics Committee of Beijing Tongren Hospital, Capital Medical University, and the Ethics Committee of Hebei Provincial Eye Hospital, and was performed in adherence to the principles of the Declaration of Helsinki. Written informed consent was obtained from all participants

Consent for publication

Written informed consent was obtained from the patients for publication of the clinical details and clinical images used in this work.

Competing interests

The authors declare that they have no competing interests.

Author details

1Beijing Institute of Ophthalmology, Beijing Ophthalmolgy and Visual Science Key Laboratory, Beijing Tongren Eye Center, Beijing Tongren Hospital, Capital Medical University, 17 Hougou Lane, Chongnei Street, Beijing 100005, People's Republic of China. 2Hebei Provincial Key Laboratory of Ophthalmology, Hebei Provincial Eye Institute, Hebei Provincial Eye Hospital, 399 East Quanbei Street, Xingtai, Hebei 054001, People's Republic of China.

References

1. Li A, Jiao X, Munier FL, Schorderet DF, Yao W, Iwata F, et al. Bietti crystalline corneoretinal dystrophy is caused by mutations in the novel gene CYP4V2. Am J Hum Genet. 2004;74:817–26.
2. Astuti GD, Sun V, Bauwens M, Zobor D, Leroy BP, Omar A, et al. Novel insights into the molecular pathogenesis of CYP4V2-associated Bietti's retinal dystrophy. Mol Genet Genomic Med. 2015;3:14–29.
3. Bietti GB. Ueber familiares Vorkommen von "Retinitis punctata albescens" (verbunden mit "Dystrophia marginaliscristallinea cornea"): Glitzern des Glaskörpers und anderen degenerativen Augenveränderungen. Klin Monatsbl Augenheilkd. 1937;99:737–56.
4. Bietti GB. Su alcune forme atipiche o rare di degenerazione retinica (degenerazioni tappetoretiniche e quadri morbosi similari). Boll Oculist. 1937;16:1159–244.

5. Mataftsi A, Zografos L, Millá E, Secrétan M, Munier FL. Bietti's crystalline corneoretinal dystrophy: a cross-sectional study. Retina. 2004;24:416–26.
6. Oishi A, Oishi M, Miyata M, Hirashima T, Hasegawa T, Numa S, et al. Multimodal imaging for differential diagnosis of Bietti crystalline dystrophy. Ophthalmol Retina. 2018;2(10):1071–7. doi:10.1016/j.oret.2018.02.012.
7. Wang W, Chen W, Bai XY, Chen L. Multimodal imaging features and genetic findings in Bietti crystalline dystrophy. BMC Ophthalmol. 2020;20:331.
8. Gocho K, Kameya S, Akeo K, Kikuchi S, Usui A, Yamaki K, et al. High-resolution imaging of patients with Bietti crystalline dystrophy with CYP4V2 mutation. J Ophthalmol 2014; 2014:283603.
9. Meng XH, He Y, Zhao TT, Li SY, Liu Y, Yin ZQ. Novel mutations in CYP4V2 in Bietti corneoretinal crystalline dystrophy: Next-generation sequencing technology and genotype-phenotype correlations. Mol Vis. 2019;25:654–62.
10. Jiao X, Li A, Jin ZB, Wang X, Iannaccone A, Traboulsi EI, Gorin MB, Simonelli F, Hejtmancik JF. Identification and population history of CYP4V2 mutations in patients with Bietti crystalline corneoretinal dystrophy. Eur J Hum Genet. 2017;25(4):461–71.
11. Yin X, Yang L, Chen N, Cui H, Zhao L, Feng L, et al. Identification of CYP4V2 mutation in 36 Chinese families with Bietti crystalline corneoretinal dystro-phy. Exp Eye Res. 2016;146:154–62.
12. Song Y, Mo G, Yin G. A novel mutation in the CYP4V2 gene in a Chinese patient with Bietti's crystalline dystrophy. Int Ophthalmol. 2013;33:269–76.
13. Raoof N, Vincent AL. Novel gene mutation in a patient with Bietti crystalline dystrophy without corneal deposits. Clin Exp Ophthalmol. 2017;45:421–4.
14. Oishi A, Oishi M, Miyata M, Hirashima T, Hasegawa T, Numa S, Tsujikawa A. Multimodal imaging for differential diagnosis of Bietti crystalline dystrophy. Ophthalmol Retina. 2018;2(10):1071–7.
15. Toto L, Carpineto P, Parodi MB, Di Antonio L, Mastropasqua A, Mastropasqua L. Spectral domain optical coherence tomography and in vivo confocal microscopy imaging of a case of Bietti's crystalline dystrophy. Clin Exp Optom. 2013;96:39–45.
16. Yokoi Y, Sato K, Aoyagi H, Takahashi Y, Yamagami M. NakazawaM. A novel compound heterozygous mutation in the CYP4V2 gene in a japanese patient with Bietti's crystalline corneoretinal dystrophy. Case Rep Ophthalmol. 2011;2:296–301.
17. Mansour AM, Uwaydat SH, Chan CC. Long-term follow-up in Bietti crystalline dystrophy. Eur J Ophthalmol. 2007;17:680–2.
18. Lockhart CM, Smith TB, Yang P, Naidu M, Rettie AE, Nath A, et al. Longitudinal characterisation of function and structure of Bietti crystalline dystrophy: report on a novel homozygous mutation in CYP4V2. Br J Ophthalmol. 2018;102:187–94.
19. Ipek SC, Ayhan Z, Kadayifcilar S, Saatci AO. Swept-source optical coherence tomography angiography in a patient with Bietti crystalline dystrophy followed for ten years. Turk J Ophthalmol. 2019;49:106–8.

20. Lee KY, Koh AH, Aung T, Yong VH, Yeung K, Ang CL, Vithana EN. Characterization of Bietti crystalline dystrophy patients with CYP4V2 mutations. Invest Ophthalmol Vis Sci. 2005;46:3812–6.
21. Holladay JT. Proper method for calculating average visual acuity. J Refract Surg. 1997;13:388–91.
22. Yuzawa M, Mae Y, Matsui M. Bietti's crystalline dystrophy. Ophthalmic Paediatr Genet. 1986;7:9–20.
23. Li Q, Li Y, Zang X, Xu Z, Zhu X, Ma K, et al. Utilization of fundus autofluorescence, spectral domain optical coherence tomography, and enhanced depth imaging in the characterization of Bietti crystalline dystrophy in different stages. Retina. 2015;35:2074–84.
24. Fong AM, Koh A, Lee K, Ang CL. Bietti's crystalline dystrophy in Asians: clinical, angiographic and electrophysiological characteristics. Int Ophthalmol. 2009;29:459–70.
25. Rossi S, Testa F, Li A, Iorio VD, Zhang J, Gesualdo C, et al. An atypical form of Bietti crystalline dystrophy. Ophthalmic Genet. 2011;32:118–21.
26. Miyata M, Oishi A, Hasegawa T, Ishihara K, Oishi M, Ogino K, et al. Choriocapillaris flow deficit in Bietti crystalline dystrophy detected using optical coherence tomography angiography. Br J Ophthalmol. 2018;102(9):1208–12.
27. Halford S, Liew G, Mackay DS, Sergouniotis PI, Holt R, Broadgate S, et al. Detailed phenotypic and genotypic characterization of bietti crystalline dystrophy. Ophthalmology. 2014;121(6):1174–84.
28. Chen H, Zhang M, Huang S, Wu D. Functional and clinical findings in 3 female siblings with crystalline retinopathy. Doc Ophthalmol. 2008;116:237–43.
29. Liu DN, Liu Y, Meng XH, Yin ZQ. The characterization of functional disturbances in Chinese patients with Bietti's crystalline dystrophy at different fundus stages. Graefes Arch Clin Exp Ophthalmol. 2012;250:191–200.
30. Nakano M, Kelly EJ, Wiek C, Hanenberg H, Rettie AE. CYP4V2 in Bietti's crystalline dystrophy: ocular localization, metabolism of omega-3-polyunsaturated fatty acids, and functional deficit of the p.H331P variant. Mol Pharmacol. 2012;82(4):679–86.
31. Rossi S, Testa F, Li A, Yaylacioglu F, Gesualdo C, Hejtmancik JF, Simonelli F. Clinical and genetic features in Italian Bietti crystalline dystrophy patients. Br J Ophthalmol. 2013;97(2):174–9.
32. Saint-Geniez M, Kurihara T, Sekiyama E, Maldonado AE, D'Amore PA. An essential role for RPE-derived soluble VEGF in the maintenance of the choriocapillaris. Proc Natl Acad Sci U S A. 2009;106:18751–6.
33. Jin ZB, Ito S, Saito Y, Inoue Y, Yanagi Y. Nao-i N. Clinical and molecular findings in three Japanese patients with crystalline retinopathy. Jpn J Ophthalmol. 2006;50:426–31.
34. Broadhead GK, Chang AA. Acetazolamide for cystoid macular oedema in Bietti crystalline retinal dystrophy. Korean J Ophthalmol. 2014;28:189–91.

Figures

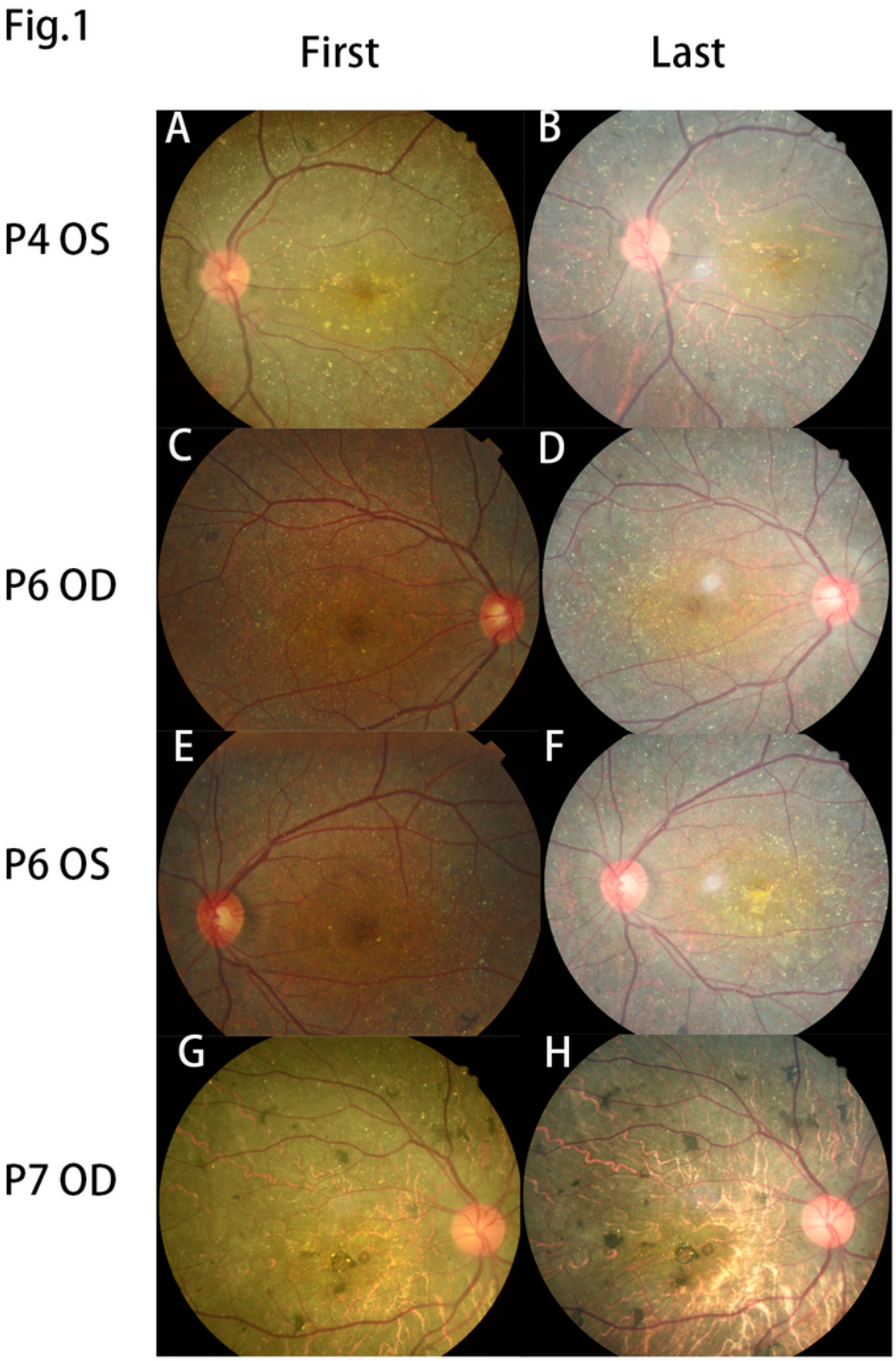

Figure 1

Fundus color photographs from the first and last visits of a patient with BCD. A, B Choroidal great vessels show more clearly than before. C, D The RPE-choriocapillaris complex atrophy of the macular area showed no significant changes, but the RPE-choriocapillaris complex of the area around the macular area was more atrophied than before. E, F A scar cause by choroidal neovascularization was observed at the

macular area, which was not apparent at the first visit. G, H The degree of pigment clumping had increased and the choroidal great vessels showed more clearly than at the first visit.

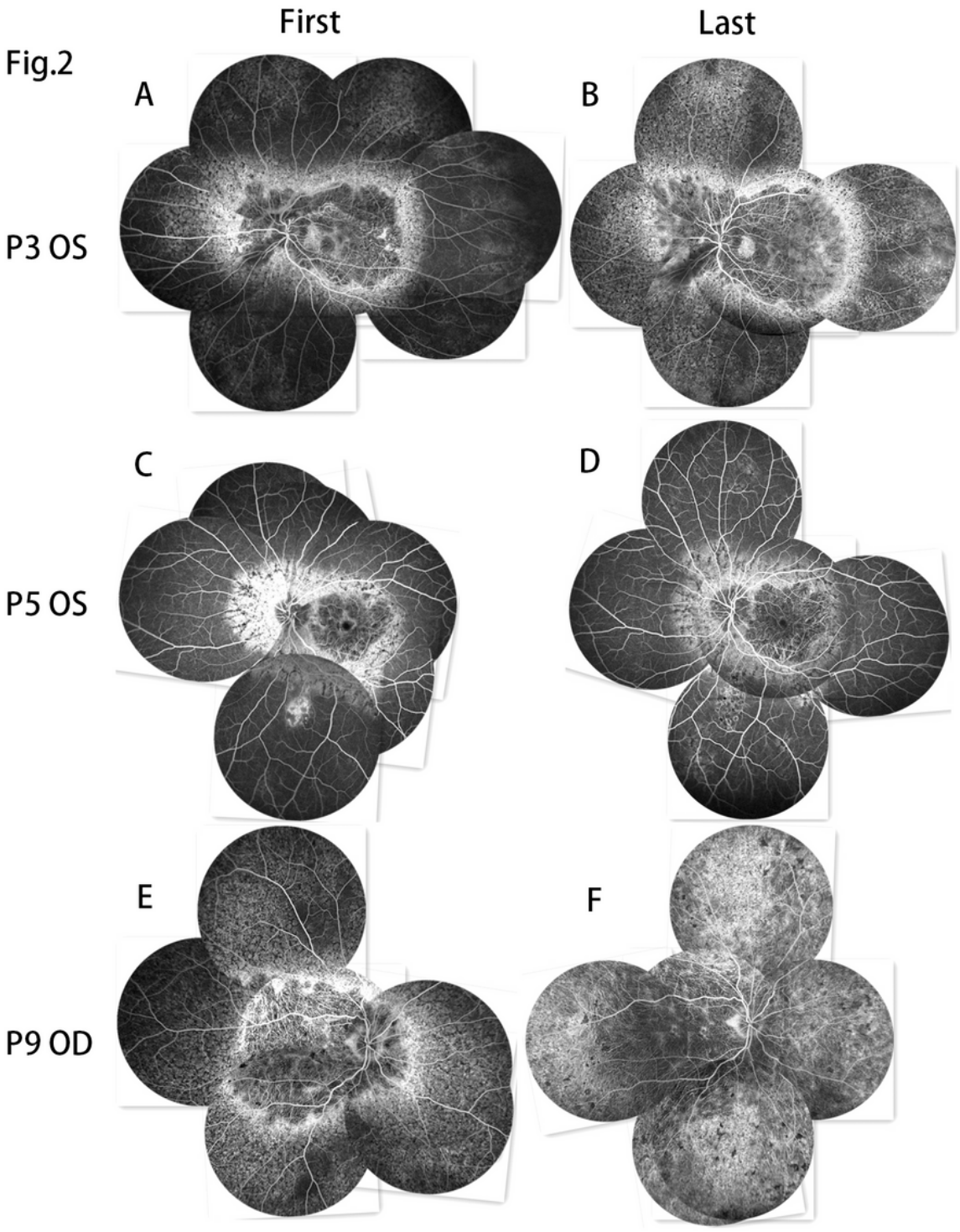

Figure 2

FFA image jigsaws of the first and last visits of P3, P5, and P9. A, B The lesion had expanded to the mid-periphery from the posterior pole and periphery. C, D As the posterior pole lesion developed, new lesions

appeared in the periphery. E, F The RPE-choriocapillaris complex showed significant atrophy since the first visit; the border of the choriocapillaris atrophy and RPE atrophy was not as clear as at the first visit.

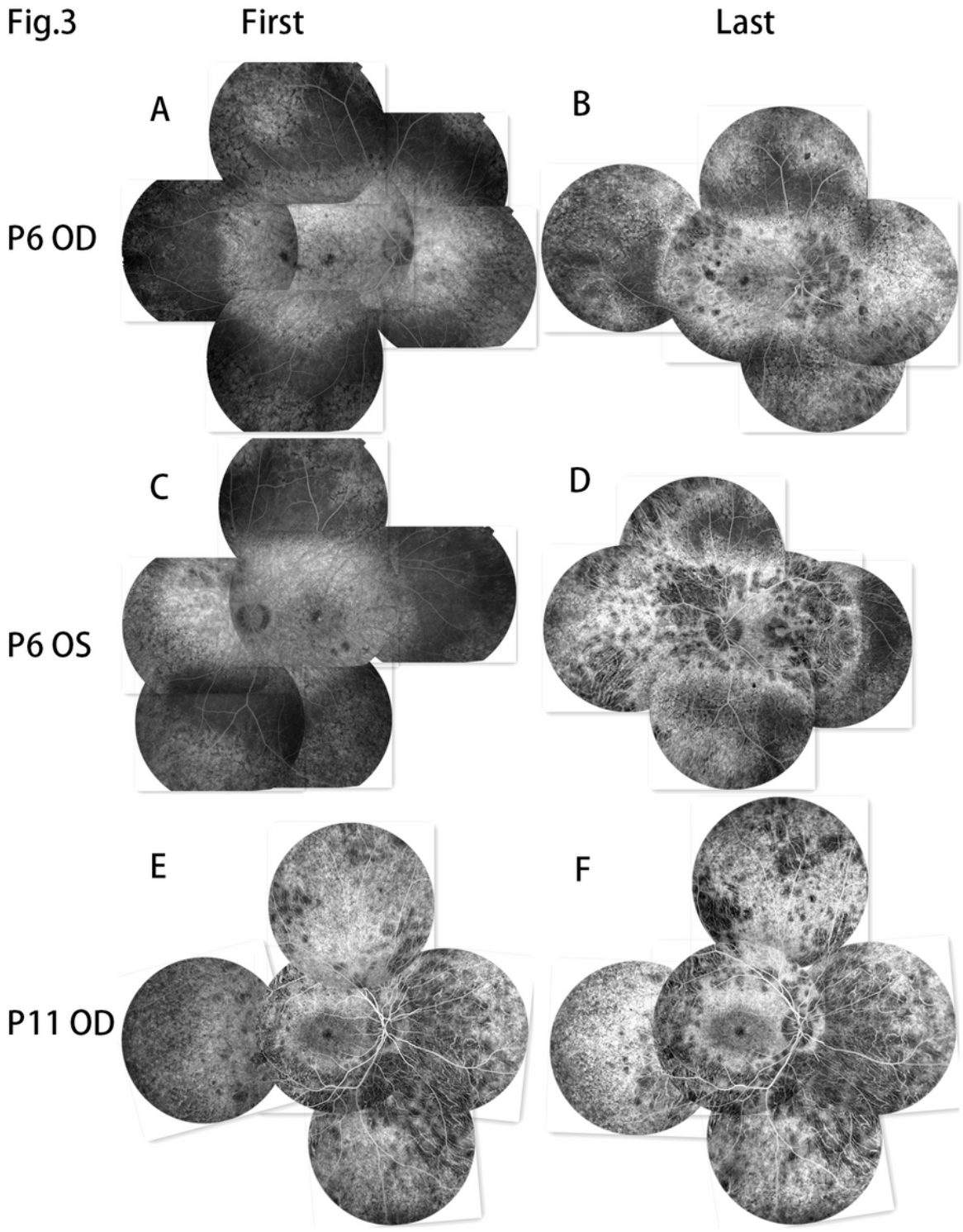

Figure 3

FFA image jigsaws of the first and last visits of P6 and P11. A, C At the first visit, both eyes of P6 showed RPE atrophy at the posterior pole, the nasal side of the optic disc, and the periphery. B, D At the last visit, the posterior and peripheral lesion had expanded to the mid-periphery, and patches of choriocapillaris

atrophy appeared at the nasal side of optic disc, the periphery, and along the superior and inferior vascular arcades. A choroidal neovascularization scar was seen at the macular area of the left eye of P6, with annular hypo-fluorescence around it. E, F The RPE atrophy of the macular area showed no significant change, but the atrophy of the rest of the fundus area showed marked changes.

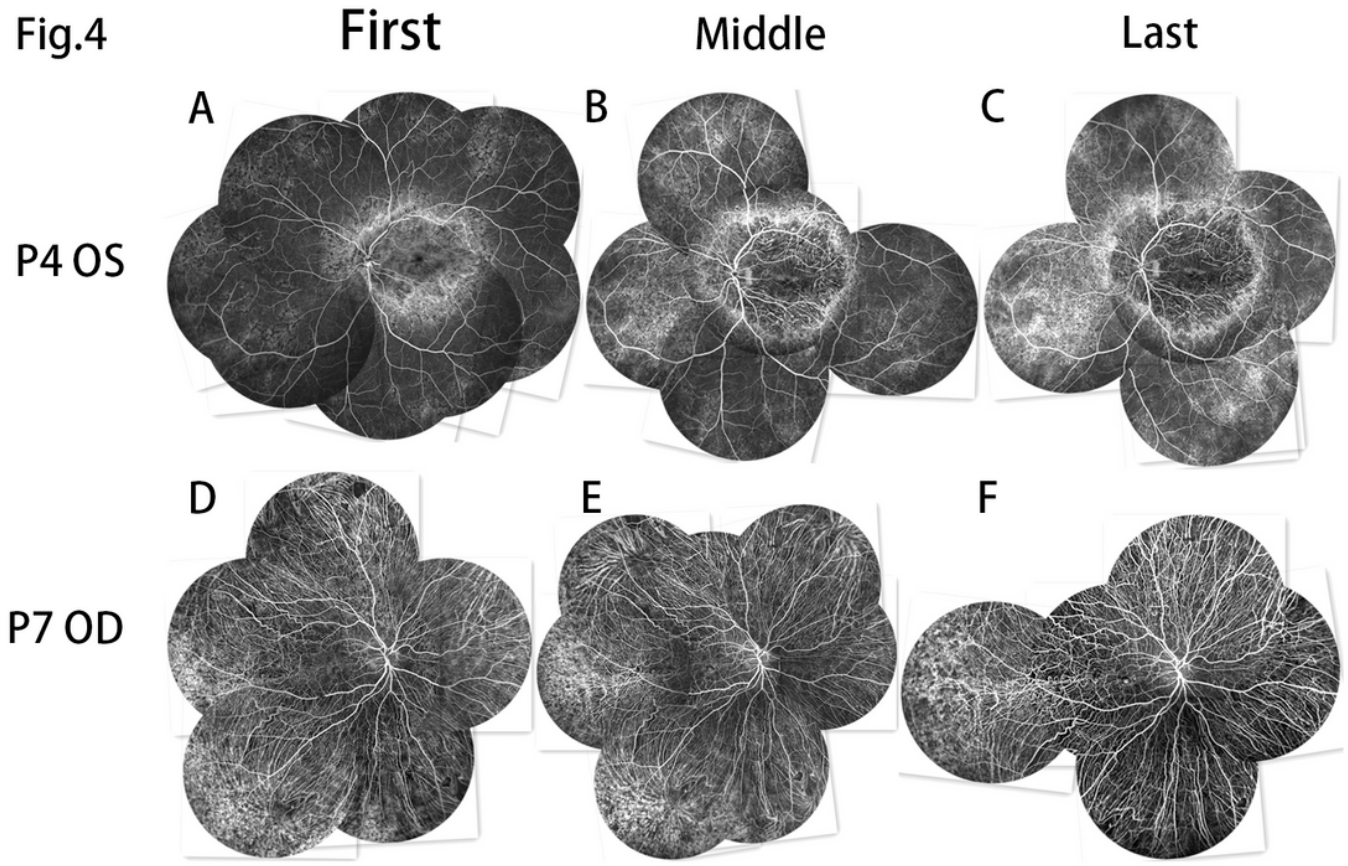

Figure 4

FFA image jigsaws of the first and last visits of P4 and P7. A, B, C Three FFA image jigsaws of the left eye of P4 taken at two-year intervals. The lesion had expanded to the mid-peripheral retina from the posterior pole retina and peripheral retina. D, E, F Three FFA image jigsaws of the right eye of P7 taken at two-year intervals. The majority of the choriocapillaris had atrophied. The remaining temporal peripheral choriocapillaris showed further atrophy over time.